Materials Science & Engineering C 107 (2020) 110210

Contents lists available at ScienceDirect

Materials Science & Engineering C

journal homepage: www.elsevier.com/locate/msec

The biocompatibility of silver and nanohydroxyapatite coatings on titanium dental implants with human primary osteoblast cells

Ranj Nadhim Salaie[a,c], Alexandros Besinis[a,b,c], Huirong Le[d,1], Christopher Tredwin[c], Richard D. Handy[a,e,*]

[a] School of Biological and Marine Sciences, Faculty of Science and Engineering, University of Plymouth, UK
[b] School of Engineering, Faculty of Science and Engineering, University of Plymouth, UK
[c] Plymouth University Peninsula Schools of Medicine and Dentistry, University of Plymouth, UK
[d] School of Mechanical Engineering and Built Environment, College of Engineering and Technology, University of Derby, UK
[e] Visiting Professor, Department of Nutrition, Cihan University-Erbil, Kurdistan Region, Iraq

ARTICLE INFO

Keywords:
Implant coatings
Clinical safety
Metal toxicity
Dissolution
Amalar blue assay

ABSTRACT

Silver nanoparticles (Ag NPs) are antimicrobial, with potential uses in medical implants, but Ag NPs alone can also be toxic to mammalian cells. This study aimed to enhance the biocompatibility of Ag NP-coated titanium dental implants with hydroxyapatite (HA) applied to the surface. Ti6Al4V discs were coated with Ag NPs, Ag NPs plus HA nanoparticles (Ag + nHA), or Ag NPs plus HA microparticles (Ag + mHA). The stability of coatings was explored and the biocompatibility with primary human osteoblasts over 7 days. Results showed that Ti6Al4V discs were successfully coated with silver and HA. The primary particle size of nHA and mHA were 23.90 ± 1.49 nm and 4.72 ± 0.38 μm respectively. Metal analysis showed that underlying silver coatings remain stable in DMEM culture media, but the presence of FBS in the media caused some initial (clinically beneficial) release of dissolved silver. With additions of HA, osteoblasts were adherent, had normal morphology, negligible lactate dehydrogenase (LDH) leak, and showed alkaline phosphatase (ALP) activity. Cell viability was around 70% throughout the Ag + nHA treatment. Overall, the implants coated with Ag + nHA maintained a higher degree of biocompatibility compared to those coated with Ag + mHA, or Ag NPs alone, suggesting the former has a benefit for clinical use.

1. Introduction

The use of titanium dental implants is becoming widely accepted amongst dentists and patients as a method of replacing teeth. Dental implants have advantages over traditional dentures including their durability, comfort and convenience for the patient. However occasionally implants fail, and while the failure rates are modest (about 7% [1]), the prospect of further surgery is a concern for patients. Thus achieving success at the first attempt of implantation is preferable. The reasons for implant failure include mechanical overload on the surrounding bone, poor wound healing or osseointegration of the implant after surgery, or infection around the implant [2]. Of these problems, bacterial infection on and around the implant (peri-implantitis) is the most common cause of failure [3,4]. The metabolic acids produced by the microbes in the somewhat anaerobic conditions of the wound, and the inflammatory response of the patient, can also prevent osseointegration [3]. Subsequently the implant becomes loose, and/or for infection control, needs to be removed.

To reduce the risk of peri-implantitis, dental implants are sterilised and the bone cavity maybe disinfected during surgery with chlorhexidine or similar agents. However, such approaches provide only temporary infection control and so research effort has focussed on coating the implant surface with antibacterial agents that provide longer lasting protection. These have included doping the implant with antibiotics such as gentamycin or disinfectants like chlorhexidine [5,6]. However, traditional antibiotics tend to target selected species of microbes and the problem of antibiotic resistance is a concern. Alternatively, agents like chlorhexidine may kill a broader spectrum of microbial species, but also damage the surrounding cells. More recently, attention has turned to the antimicrobial properties of engineered nanomaterials, especially Ag NPs that are known to be a good antimicrobial [7]. Besinis et al. [8] demonstrated that dentine discs coated with Ag NPs provided a stable

* Corresponding author. School of Biological and Marine Sciences, Faculty of Science and Engineering, University of Plymouth, UK.
E-mail address: r.handy@plymouth.ac.uk (R.D. Handy).
[1] The Future Lab, Tsinghua University, Beijing, China.

https://doi.org/10.1016/j.msec.2019.110210
Received 25 February 2019; Received in revised form 30 August 2019; Accepted 16 September 2019
Available online 30 October 2019
0928-4931/

biomaterial that was effective at preventing growth of *Streptococcus mutans*. Several authors have also attempted to incorporate silver onto the surface of medical grade titanium alloy. For example, Besinis et al. (2017) [9] found that a nano silver coating on titanium dental implants can have potential antibacterial activity against *Streptococcus sanguinis in vitro* and prevented biofilm formation.

However, silver is also toxic to mammalian cells [7], including the fibroblasts involved in wound healing where the lethal concentration of $AgNO_3$ is 50 mg L^{-1} [10]. Ag NPs are also toxic to cells *in vitro* (EC_{50} 26.7 mg L^{-1}), [11]. Thus, there is a concern that the addition of Ag NPs to provide antibacterial properties to the dental implant, may concomitantly undermine its biocompatibility with human tissue. Biocompatibility with the osteoblasts that are central to the osseointegration of the implant into the surrounding bone is a particular concern. Ideally, an implant should have enough Ag NPs to be antimicrobial for several days after surgery to help minimise the risk of post-operative infection, but also promote osseointegration. However, the precise concentrations of Ag NPs that are biocompatible with osteoblasts are poorly understood.

One approach to resolving this dilemma is to make a composite material where the different components promote antimicrobial activity and biocompatible properties respectively. For the latter, synthetic HA is well-known to simulate the mineral properties of natural bone, and is regarded as a biocompatible and osteoconductive material [12,13]. Traditional micron scale HA has been used for some years to enhance the biocompatibility of bone implants [14]. However, the surface topography of the material is important when considering interactions with osteoblasts, and more recently nanoscale HA has been given much attention [15]. Nano HA can improve osteoblast cell adhesion to the implant surface, promote bone cell proliferation and their subsequent calcium deposition to make new bone, compared to the traditional micron scale HA [16].

There are two fundamental approaches to the synthesis of Ag-HA composites on medical grade Ti alloy. The first involves growing a layer of biocompatible material on the surface of the alloy, for example micron-scale HA [17], or a material with topography that promotes osteoblast adhesion such as TiO_2 nanotubes [18]. Then, this biocompatible layer can be covered with Ag NPs (e.g., by reduction of a silver solution). Having the silver as the uppermost layer offers a biocidal advantage. Any dissolved silver released from the coating will be directly toxic to microbes. In the case of Ag NPs, both metal dissolution from the particles and direct contact of the particles with microbes can be toxic [7,8]. However, there remains a problem in that the osteoblast cells have limited access to their preferred substrate (i.e., the HA) underneath the silver layer.

The alternative approach is to coat the Ti alloy with silver, and then add a layer of biocompatible HA. The silver coating is typically achieved by electroplating and depending on the silver solutions, voltage and temperature used; either an amorphous silver layer or Ag NPs [9] may be grown on the surface. Then either a micron- or nano-HA can be added as a final coating. Crucially, our previous studies showed that provided the HA coating has some porosity (i.e., spaces in between the HA particles), then the antibacterial properties of the silver layer is retained, killing the microbes within 24 h [9].

Here, the same type of Ag-HA composites we used previously to demonstrate antimicrobial properties [9] are explored further for their biocompatibility with human osteoblast cells *in vitro*. The overall aim was to demonstrate that healthy osteoblast will grow on the composite material. The specific objectives included examining the morphology of osteoblasts on the composite by electron microscopy, and then assessing indicators of cell health. For the latter, electrolyte composition of the cells and lactate dehydrogenase activity (LDH leak) were measured. The presence of alkaline phosphatase activity which is functionally important to the ability of the cells to make bone was also determined. The stability of the coatings were also explored by following Ca^{2+}, P and Ag release into the cell culture media, and the maximum dissolution rate of silver determined in order to know if any dissolved fraction of presumably toxic silver ions were released.

2. Materials and methods

The experimental approach consisted of coating medical grade titanium alloy with a Ag NP surface to provide an antibacterial coating, with the subsequent addition of an HA covering to enable biocompatibility with osteoblast cells. The first steps involved preparing and characterising the coatings for their morphology and integrity. Then, osteoblasts cells were seeded onto the coated discs and allowed to grow for seven days, with a range of biological endpoints measured (see below) to determine cell health and function.

2.1. Preparation and coating of medical grade titanium alloy

The titanium alloy selected for the experiments is routinely used for medical implants and the method for preparing the discs was based on [9]. Briefly, grade five titanium alloy (Ti6Al4V) discs measuring 15 mm in diameter and 1 mm thickness were prepared by laser cutting and then polished with (800–1200 grit) sand papers using a rotary instrument (Grinder-Polisher, Buehler, UK Ltd, Coventry, England). Six and one μm diamond solutions (Diamond solution, Kemet International Ltd, UK) were used for the final polish. The discs were subsequently cleaned with an alkaline solution and 5% HCl as previously described [9]. The cleaned titanium discs were then coated with Ag NPs by an electroplating method.

Briefly, the clean titanium discs were hung on silver or platinum wires connected to the cathode of a voltage supply (BK Precision, 9174 DC power supply), while a fine silver sheet (1 mm thickness, 50 mm × 100 mm, Cooksongold Ltd, UK) comprised the anode. The discs and silver sheet were immersed in an electrolyte (0.2 M $AgNO_3$, 0.4 M succinimide, and 0.5 M KOH; all from Sigma Aldrich, UK) at 40 °C and the voltage was adjusted to 1 V and left for 3 min. The resulting silver plated discs were rinsed with distilled water to remove the electrolyte, air dried and then coated with nHA or mHA using a sintering technique.

The nano HA dispersion (nanoXIM.HAp102 aqueous paste, mean particle size < 50 nm, purity > 95%) was purchased from Fluidinova (Rua Eng. Frederico Ulrich 2650, 4470-605 Maia, Portugal) at a concentration of 15 % wt/v (150 g L^{-1}) dispersed in water. A 15 % wt/v dispersion of mHA was prepared by adding 15 g of HA powder (nanoXIM.HAp202, HA spray-dried powder, mean particle size is 5 ± 1 μm, supplier as above) into 100 mL of ultrapure deionised water (18.2 MΩ). The dispersion was then vortexed for 10 min. The resulting stock dispersions were then diluted in ultrapure water to 10 mg L^{-1} (nHA) and 1000 mg L^{-1} (mHA), and used for measuring primary particle size by transmission electron microscopy (TEM) at Plymouth University. The stock dispersions were also measured in triplicate for particle size distribution and hydrodynamic diameter using Nanoparticle Tracking Analysis (NTA, Nanosight LM 10, Nanosight, Salisbury, UK, laser output set at 30 mW at 640 nm).

The silver plated discs were individually placed in the wells of 24 well microplates (flat-bottom, sterile, polystyrene microplates, Greiner 662160, Bio-One Ltd., UK) and then 20 μl of the appropriate HA dispersion was added to the top of the discs and distributed evenly with a pipette. The discs were left in an incubator at 37 °C to dry for at least 48 hours. Finally, the specimens were transferred to porcelain dishes and placed in a furnace for sintering (Carbolite, ELF 11/14, UK). The rate of temperature increase in the furnace was 10 °C/min until 500 °C was achieved. This temperature was maintained for 10 min, subsequently the now HA and Ag coated discs were left to cool.

2.2. Characterisation of the coated titanium alloy discs

The discs were examined by scanning electron microscopy (SEM) to

determine the coverage and chemical composition of the coatings. Surface roughness measurements were also taken to confirm the nano- or micron-nature of the relevant coatings. In addition, the integrity of the coatings in ultrapure water and in different cell culture media were examined with dialysis experiments to estimate any apparent dissolved silver or HA from the coatings. For the microscopy, the silver plated, nano- and micron- HA-coated discs were examined under SEM mode (JEOL/JSM-7001F, with an Oxford Instruments INCA X-ray analysis system attached) to confirm the presence, quality, and composition of the coatings. Detective energy was 15 keV at a working distance of 10 mm. At least one disc of each type in each batch of discs prepared were examined. A thin layer of chromium was sputter coated on the specimens to increase conductivity and therefore the resolution for imaging. Moreover, qualitative and quantitative metal analysis were carried out on at least one disc of each type of fresh discs in each batch using Energy Dispersive Spectroscopy (EDS, spot size, 10 μm; accelerating voltage, 15 kV; working distance, 10 mm). The data and spectral analysis were achieved using the Aztec 2.2 software supplied with the instrument.

Surface roughness is a key attribute for the biocompatibility and osseointegration of osteoblasts. Very smooth surfaces do not promote osteoblast attachment, but equally very rough surfaces are prone to microbial biofilm formation. Moderate roughness values of around 1–2 μm (peak to valley distance) are preferred for osteoblasts [19]. The surface roughness values (Ra) were measured using an Olympus LEXT Confocal Microscope OLS 3000, with a total magnification of 50 × and an optical zoom of 1 × . Profiles were Gaussian filtered with a cut-off wavelength value of 85.2 μm using the software associated with the instrument. Surface roughness was measured at three different locations for each of the 3 replicate discs from each treatment. Following the surface roughness measurements, topographical 3D images were also collected.

2.3. Dissolution of silver and the stability of the coatings

The stability of the coatings was investigated by measuring the apparent total dissolved silver release into cell culture media, compared to ultrapure water for reference, during dialysis experiments based on the method of Handy et al. [20]. The approach measured dissolution at each step of the coating procedure and thus the experiments included a negative control (blank, with no discs), silver plated (Ag), silver plated + nano HA (Ag + nHA) and silver plated + micro HA (Ag + mHA) discs respectively. Experiments were performed in triplicate using Dulbeco's Modified Eagle's Medium (DMEM) supplemented with 10% foetal bovine serum (FBS, Invitrogen, UK) and 1% of penicillin-streptomycin (Life Technology, UK) compared to the appropriate ultrapure water controls. Briefly, acid washed beakers were filled with 246 mL of the appropriate media. The discs were individually placed in acid washed dialysis bags (product code: D9777, molecular weight cut off 12, 000 Da, pore size < 2 nm, Sigma-Aldrich Ltd, Dorset, UK) containing 4 mL of media, sealed, then suspended individually in beakers (final total volume 250 mL) and gently stirred at room temperature. Samples of the external media (5 mL) were collected at 0, 0.5, 1, 2, 3, 4, 6, 8 and 24 h for immediate pH determination and subsequent ion analysis (see below).

Initial experiments showed some apparent silver dissolution into the beakers with the DMEM media for the coated discs, and thus a further series of trials were conducted to determine what aspect of the DMEM chemistry was causing the release. This series of experiments used Ag + nHA discs in DMEM with different concentration of FBS, dilution of the DMEM with a Kreb's saline, and also with a different cell culture media (Hob cell culture medium, Culture Collections, Public Health England). The control was the Ag + nHA-coated discs in normal DMEM +10% FBS and 1% of penicillin-streptomycin, and an equivalent negative control without the disc. The experimental groups are listed (Table 1). Experiments were conducted in triplicate in sterile conditions, using sterile discs (gamma irradiated, [9]). Discs were placed in 24 well-microplates with 0.6 mL of the relevant cell culture medium, then incubated for 72 h in 5% CO_2 95% air (HETO-HOLTEN Cell House 170) at 37 °C. The media was carefully collected and replaced with fresh media every 24 h. The aliquots of media were acidified with 20 μL of 100% nitric acid for subsequent metal determination (see below). After 3 days, the experiment was terminated and the discs were rinsed in ultrapure deionised water, then prepared for SEM as described above.

2.4. Experiments with cultured human osteoblasts

The experiments were performed using primary human osteoblast cells (HOb cells) obtained from the European Collection of Cell cultures (ECACC). The cells were cultured in 75 cm^2 flasks (Sterilin, Newport, UK) with vented caps, and containing 15 mL of DMEM (Dulbecco's Modified Eagle's medium) with 10% foetal bovine serum (FBS) and 1% penicillin-streptomycin (100 IU Penicillin - 100 μg mL^{-1} Streptomycin) purchased from Invitrogen. For routine culture, the media were changed every 3–4 days, and cells were sub-cultured into new flasks when 80–85% confluence was reached. Cells were maintained at 37 °C in a humidified atmosphere of 5% CO_2 and 95% air.

The experiments were performed in 24 well-microplates (as above), with the microplate as the unit of replication in the experimental design (n = 6 plates/treatment). Briefly, 30,000 cells in 0.6 mL aliquot of the stock culture DMEM media supplemented with 10% FBS and 1% of the antimicrobial (as above) were added to each well. The treatments included cells grown on the normal microplates without any alloy discs (reference control); an uncoated titanium disc (Ti) silver plated discs (Ag), silver plated and nHA-coated discs (Ag + nHA), or silver plated discs coated with mHA (Ag + mHA). The cells were incubated with the appropriate treatment or control for 7 days in 95% air and 5% CO_2 at 37 ^{O}C. The cell culture medium was collected for biochemistry and ionic analysis (see below) and replaced with fresh media on days 1, 4 and 7.

After 7 days the cells were washed with 2 mL of a washing buffer (300 mmol L^{-1} sucrose, 0.1 mmol L^{-1} EDTA, 20 mmol L^{-1} HEPES buffered to 7.4 with few drops of trizma base) and then 1 mL of a lysis buffer was added (the same buffer as above, except hypotonic with a sucrose concentration of 30 mmol L^{-1} and containing 0.001% of Triton-X 100). The cells were homogenised for 10–15 min manually with a pipette to ensure the complete detachment of the cells from the surface. The crude cell homogenates were used for the biochemical assays, as well as silver and electrolytes determinations (see below). A final repeat of the experiment (exactly as above) was performed (n = 3 plates), but for the latter, the cells were fixed after 7 days and investigated under scanning electron microscopy for morphology (see below).

2.5. Biochemistry

Cell viability was assessed using the alamar blue assay in the cell culture plates on days 1, 4 and 7. A volume of alamar blue dye (abD Serotec, UK) equal to 10% of the cell culture medium was added to each well and the cells were incubated for 6 h in the dark. Then, 200 μL of the resulting cell culture medium from each well was transferred to a new 96 well plate and then the absorbance was measured at 600 nm (plate reader above). Cell viability was expressed as a percentage of the reference control.

Lactate dehydrogenase (LDH) activity is a well-established biomarker of membrane integrity and was measured every day in the external media to assess any leak of the enzyme from the cells, and in cell homogenates at after 7 days [21]. Briefly, 100 μL of sample (media or homogenate) was added to a reaction mixture (2800 μL of 6 mmol L^{-1} sodium pyruvate in 50 mmol L^{-1} phosphate buffer at pH 7.4, plus 100 μL of 6 mmol L^{-1} NADH solution), mixed directly in a 3 mL cuvette

Table 1
Total silver concentrations released from silver-plus nano HA-coated discs to the external media after 72 h of incubation without cells.

Treatment and Type of Media	Total Ag Concentration (mg L^{-1})		
	Day1	Day 2	Day 3
DMEM + 10% FBS without disc	< 0.03 a	< 0.03 a	< 0.03 a
Physiological saline + 10% FBS without disc	< 0.03 a	< 0.03 a	< 0.03 a
HOb without disc	< 0.03 a	< 0.03 a	< 0.03 a
DMEM + 10% FBS (Control)	18.83 ± 2.38 e	2.61 ± 0.52 c #	1.75 ± 0.11 b #
DMEM without FBS	0.07 ± 0.003 b	0.19 ± 0.04 b	0.17 ± 0.04 e
DMEM + 25% physiological saline + 10% FBS	10.82 ± 0.6 d	2.59 ± 0.29 c #	1.80 ± 0.07 b #
DMEM + 50% physiological saline + 10% FBS	10.85 ± 1.1 d	2.67 ± 0.38 c #	1.92 ± 0.17 b #
Physiological saline + 10% FBS	4.77 ± 0.96 c	7.04 ± 0.46 d	2.67 ± 0.45 c *
HOb	4.70 ± 0.54 c	1.68 ± 0.08 c #	0.96 ± 0.01 d #

Data are expressed as mean ± S.E.M ($n = 3$). Different letters within each column indicate statistically significant difference. * indicates a significant difference within the previous time point. # indicates a significant difference from day 1 (one-way ANOVA, $P < 0.05$). Note, all the treatment groups containing Dulbeco's Modified Eagle's Medium (DMEM) were supplemented with 1% antibiotics. FBS, foetal bovine serum. HOb, Human osteoblast cell culture medium.

and the change in absorbance measured over 2 min at 340 nm (Jenway 7315 spectrophotometer).

Alkaline phosphatase (ALP) activity is a functional biomarker of osteoblasts because it is essential for the mineralisation of bone. ALP activity was measured in the cell homogenates at the end of the experiment. For the cell homogenates, 30 µL of sample was added to the well of 96 well microplates, then 105 µL of 100 mmol L^{-1} glycine (pH 10), and 145 µL of 500 µmol L^{-1} para-nitrophenylphosphate (pNPP, Acros, UK) to start the reaction. The plate was shaken twice, then read immediately (VersaMax plate reader, molecular devices, Berkshire, UK) for 300 s in kinetic mode at 405 nm. Enzyme activities were normalised to cell homogenate protein content. The latter was determined in 10 µL of cell homogenate by the bicinchoninic acid (BCA) method using a commercial kit (MC155208, Pierce, Rockford, USA).

2.6. Silver and electrolyte analysis

The total concentration of Ag, Na^+, K^+, Ca^{2+} and P was determined in the DMEM media after 1, 4 and 7 days, and in the cell homogenates at the end of the experiment. The Ag measurements were made to confirm the exposure, and the electrolytes in the context of cell health. For metal and electrolyte analysis, 400 µL of the external media from each well was acidified with 20 µL of 70% nitric acid. For the cell homogenate, 800 µL from each sample was taken and acid digested with 1 mL of 70% nitric acid and left overnight for complete acid digestion. Ag, Na^+, K^+ and Ca^{2+} and P of each sample were determined using ICP-OES (iCAP 7400 RADIAL, Hemel Hempstead, UK) against matrix matched standards. Sample runs included blanks to correct for instrument drift and procedural blanks to correct for background metal concentrations.

For the dialysis and dissolution experiments, the total concentration of silver was determined by inductively coupled plasma mass spectrometry ICP-MS (X series, 0475, UK) in acidified samples. For the dialysis experiment, 0.1 mL of 70% nitric acid was added to 5 mL of the samples. For the dissolution experiment with the discs, 0.02 mL of 70% nitric acid was added to the appropriate media. Sample blanks and matrix matched standards were used as above.

2.7. Morphology and confluence of cells grown on the coatings

Scanning electron microscopy was also used to visualise the morphology of osteoblasts at the end of the experiment (day 7). Cells were examined *in situ* on the discs. The cells were fixed with 1 mL of 2.5% glutaraldehyde in sodium cacodylate buffer, then immersed in a series of ethanol solutions (30, 50, 70, and 95%) for 20 min each then 100% ethanol for 1 h, 50% ethanol - 50% hexamethyldisilazane (HMDS) solution for 30 min, and finally 100% of HMDS for 60 min. The specimens were air dried overnight and sputtered with gold. Cells from each triplicate per treatment were examined for morphology, including the presence of a normal cell membrane without membrane blebs, presence of dorsal ruffles as well as the usual presence of filopodia and the stellate appearance of actively growing osteoblasts.

2.8. Statistical analysis

All data are expressed as mean ± standard error of the mean (S.E.M.) and were analysed using Statgraphics (version 16). To investigate differences between the treatments or within the treatment at different time points, the values were subjected to a one-way analysis of variance (ANOVA) using the Tukey test to locate any differences. For non-parametric data, the Kruskal Wallis test was used for the data that were not normally distributed, with the locations of any differences visualised using Box and Whisker plots. In addition, to check if there was an overall treatment x time effect, two-way ANOVA was used. Values of $P < 0.05$ were considered as a significant difference. The curves obtained from the dialysis experiment were fitted using SigmaPlot 12.0 (Systat Software, Inc).

3. Results

3.1. Characterisation of titanium alloy discs

Initial TEM studies evaluated the primary particle size and morphology of the stock dispersions of each material (Fig. 1), and confirmed the primary particle size of the nHA and mHA as supplied. The nHA had the expected rod-like morphology with an average dimension of 25.9 ± 1.6 nm in length and 13.59 ± 1.4 nm in width. The mHA were spherical with an average diameter of 4.72 ± 0.38 µm (Fig. 1). Nanoparticles tracking analysis showed that the hydrodynamic diameters of aggregates in the stock dispersions were (mean and S.E.M., $n = 3$) 326.6 ± 16.1 nm and 853.3 ± 185.1 nm for nHA and mHA respectively.

After the coatings were prepared on the titanium alloy discs the surface roughness, morphology and chemical composition were measured prior to experiments with osteoblasts. Surface roughness values were (mean ± S.E.M., $n = 3$): 0.2 ± 0.01, 0.27 ± 0.01, 0.74 ± 0.14, and 1.25 ± 0.02 µm for polished titanium discs, Ag plated titanium, Ag + nHA and Ag + mHA discs respectively. There were no statistical differences in surface roughness between the polished and electroplated discs, demonstrating that the electroplating did not add roughness to the surface. However, an increased roughness was observed with the addition of both nHA or mHA compared to either disc prior to HA addition. The mHA, as expected, produced the roughest coating (one-way ANOVA $P < 0.05$).

Scanning electron microscopy images showed that the coatings were successfully applied to the discs (Fig. 2). The silver-coated titanium disc

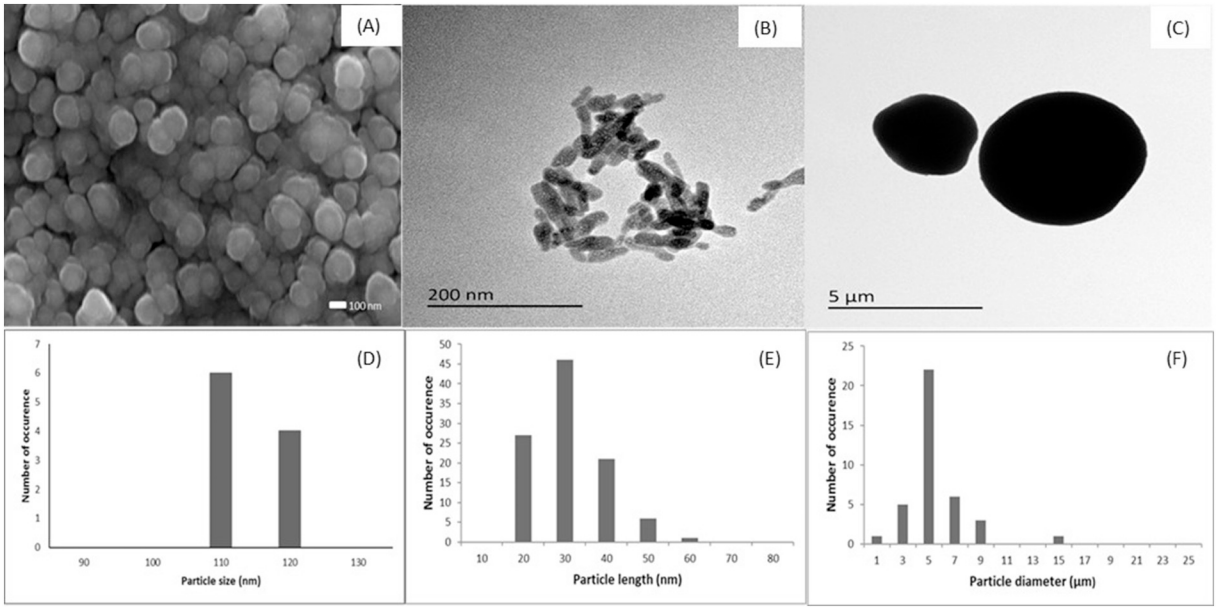

Fig. 1. (A) Scanning electron micrograph (SEM) image of electroplated Ag NPs showing the primary particle size around 111 nm. Panels (B) and (C) show transmission electron micrograph (TEM) images of hydroxyapatite nanoparticles (nHA) and microparticles (mHA), with their primary particle size (scale bars are 200 nm and 5 µm respectively). The nHA was rod-like in shape (25.95 nm in length by 13.59 nm in width) and the mHA was roughly spherical with a diameter of about 4 µm. D, E and F are the primary particle size distributions of silver, nHA stock solution and mHA stock solution. The samples from the stock solutions were dried and checked under TEM, and then the particle size was measured.

showed a uniform layer of silver at the nano scale. The Ag + nHA samples were also coated uniformly with a densely packed layer of HA nanoparticles, although some cracks occurred which probably arose from the sintering process. The mHA particles were successfully coated onto the silver-coated titanium discs without cracking (Fig. 2).

The EDS analysis (Fig. 2) confirmed the expected surface composition of the discs. The surface composition of silver-coated samples was mainly silver (78%), followed by oxygen (16%), and titanium (3%). Moreover, the surface of the Ag + nHA samples were mostly composed of calcium (31.2%) followed by phosphorous (13.8%) and silver (8.9%); confirming that most of the silver was covered by the layer of nHA. In contrast, in the Ag + mHA discs the surface had more silver (28.6%), and slightly less calcium (22.6%) and phosphorous (9.8%). For the mHA, the large particles enabled gaps between the particles where the silver coating could be observed.

3.2. Investigating the stability of the silver coating in cell culture medium

A dialysis experiment was conducted to investigate the stability of the coatings in DMEM cell culture medium (DMEM + 10%FBS + 1% antibiotics) compared to ultrapure water (Fig. 3). In the case of the titanium alloy coated with Ag NPs alone, the release of total dissolved Ag into the external compartment of the beakers was negligible ($< 1\ \mu g\ L^{-1}$) in both ultrapure water and cell culture media. However, the presence of HA on the coatings increased the release of dissolved silver from the discs. In the latter cases, the release was greater in ultrapure water compared to cell culture media (Fig. 3). However, in both cases the release over 24 h was still only $20\ \mu g\ L^{-1}$ of Ag or much less. The maximum dissolution rate for Ag + mHA was 2.24 and $0.54\ \mu g\ min^{-1}$ in ultrapure water and in cell culture media respectively. It was not possible to express the release as a percentage of the silver present as the depth of Ag on the coating could not be quantified. However most of the Ag (mg L^{-1} amounts), remained trapped inside the dialysis bag, presumably in particulate form (Fig. 3C). Regardless, the Ag + mHA coating leached the most total dissolved Ag, fitting the observations of the gaps between the mHA particles (Fig. 2) such that the external media could access the silver layer.

An additional trial with various modifications of DMEM attempted to identify the cause of the apparent silver dissolution (Table 1). DMEM +10%FBS +1% antibiotics (as a control media) caused significantly higher silver dissolution ($18.83 \pm 2.38\ mg\ L^{-1}$) after one day from brand new discs as compared to the other discs (one-way ANOVA $P < 0.05$); but this silver release to the media decreased with each daily change of the external solution. Dilution of the DMEM with physiological saline had no effect on the apparent silver release at any time point. However, DMEM with FBS caused significantly more elevation of total silver in the media compared to that without FBS, indicating that FBS may enhance the silver release. HOb media caused significantly less silver dissolution than other groups containing DMEM and FBS at day 1, although both types of media were around $4\ mg\ L^{-1}$ of total silver. At day 2 and 3, silver concentration in physiological saline +10% FBS was significantly higher than other groups (Table 1), suggesting less silver leaches in culture media(s) than simple saline.

3.3. Silver release to the external media and exposure to the cell monolayer

Results of this study with the cells present showed that there was a consistent silver release (around $2\ mg\ L^{-1}$) from the silver-coated titanium discs to the external media (Table 2). The silver concentrations in the cell culture media of the reference control and Ti alone was negligible (as expected); and low in the nHA and mHA compared to the intended silver-containing coatings in all the time points (one-way ANOVA, $P < 0.05$). The silver concentration in the Ag, Ag + nHA and Ag + mHA increased at day 4 and 7; with the highest silver release from the Ag + mHA treatment at day 4 ($7.002 \pm 2.375\ mg\ L^{-1}$, Table 2). There were no significant differences between the silver-coated groups (Ag, Ag + nHA and Ag + mHA) at any time points, also, no significant difference (one-way ANOVA, $P > 0.05$) was observed between time points within the same treatment (Table 2). However, a two-way ANOVA showed that both factors (time and treatment) have a significant effect on silver release ($P < 0.05$).

The exposure of the cells to silver was also confirmed by the concentration of silver in the cell homogenates, which was less than $10\ \mu g\ min^{-1}\ mg^{-1}$ protein (Fig. 4A). There was no evidence of altered

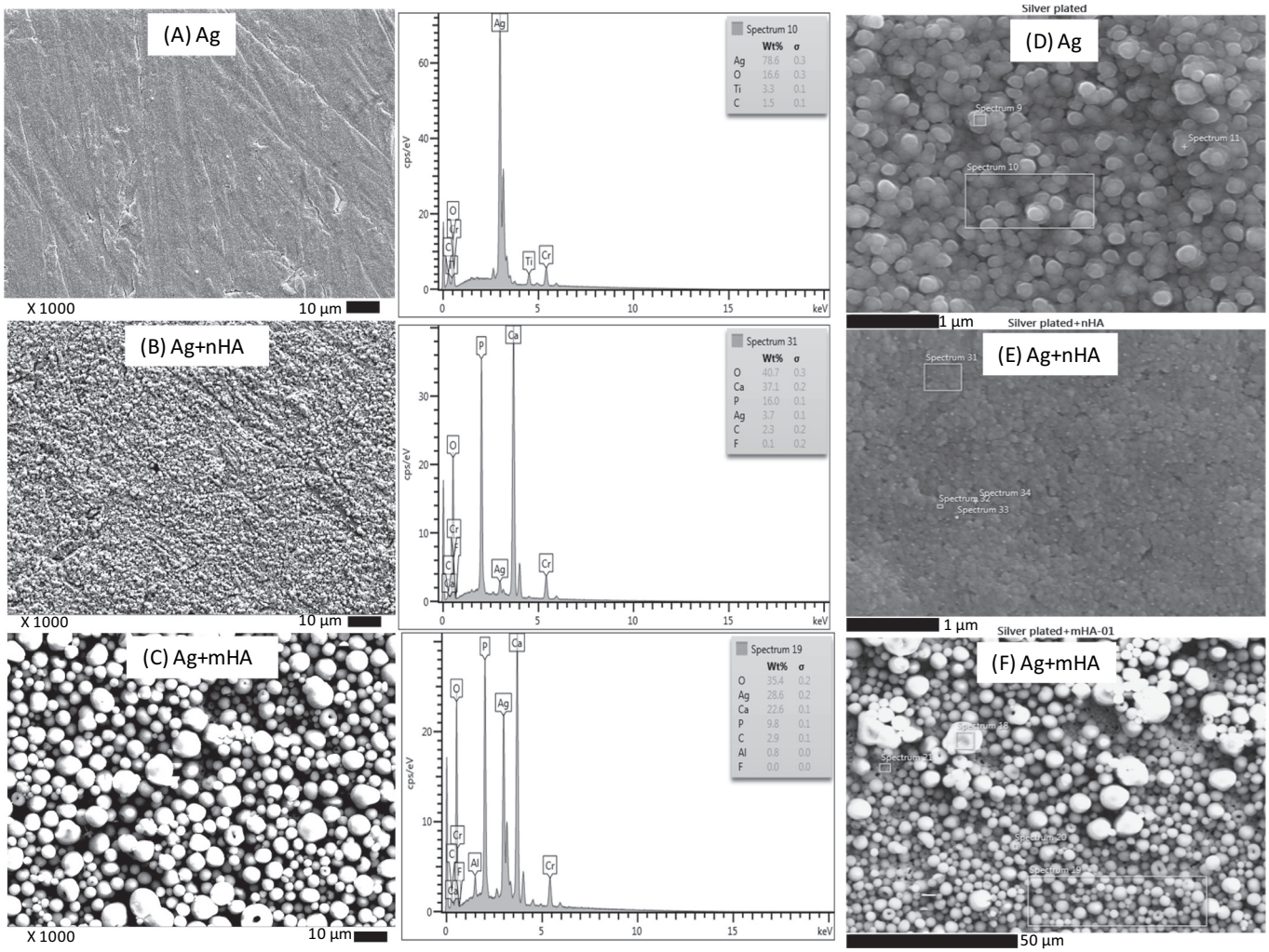

Fig. 2. SEM images of coated titanium discs; (A) silver plated titanium alloy disc surface, (B) Ag + nHA disc surface, (C) Ag + mHA disc surface. Note the particles in (A) and (B) are at the nano scale and fully covering the titanium surface. Both the nHA and mHA particles have been successfully coated on to the silver plated titanium, but the geometry of the mHA is less even. SEM images on the right show the area scanned by energy dispersive spectroscopy (EDS) and the corresponding spectra with the percentage elemental composition of the surface of coated titanium discs: (D) silver plated titanium, (E) Ag + nHA and (F) Ag + mHA.

electrolyte balance in the cells that might be associated with exposure to dissolved silver (Fig. 4B). There was no significant difference in the Na^+ or K^+ concentration between the treatments (one-way ANOVA, $P < 0.05$) and values were between 15-35 and 5–15 µmol mg^{-1} protein for Na^+ and K^+ respectively (Fig. 4B).

3.4. Osteoblast morphology

Osteoblast cells were examined under SEM after 7 days of the experiment (Fig. 5). Images showed that the cells grown on the titanium, alloy discs without any HA or silver (Ti only) were attached to the substrate and covered most of the surface (Fig. 5A). The Ti-treated cells also appeared healthy without any noticeable membrane rupture or blebs. The cells from this treatment were confluent and there were no visible signs of cellular shrinkage. Cells grown on nHA and mHA treatments were also confluent, and appeared attached to the substrate and with each other. There was no visual evidence of membrane damage in these latter cells. The level of confluence was higher in nHA compared to mHA (Fig. 5E and F). In contrast, cells grown on the Ag-coated Ti alloy discs were more sparse. However, the cells that were present did not show overt pathology, with the absence of membrane blebs on the cell membrane, and no evidence of rupture of the membrane. The cells still showed the typical extending filopodia of osteoblasts, although shrinkage was noticed in some of these cells (Fig. 5B). The cells grown on the Ag + nHA discs were almost 90% confluent, and appeared to be attached to the surface and to each other. There was no noticeable sign of cell membrane damage and no noticeable evidence of cell shrinkage (Fig. 5C). Cells on the Ag + mHA discs exhibited similar characteristics with those grown on Ag. The cells from the Ag + mHA treatment were the most sparse, and with poor contact with each other despite having filopodia (Fig. 5D). There was noticeable cell shrinkage, but there was no morphological evidence of cell membrane damage in the Ag + mHA treatment.

3.5. Cell viability and enzyme activities

The alamar blue assay was used to assess cell viability at days 1, 4 and 7 (Fig. 6). The Ti control showed around 100% viability at all time points (Fig. 6A), consistent with the observed normal morphology (Fig. 5). Cell viability in the nHA treatment was higher than 80%, and not significantly different from the Ti or silver plated groups (one-way ANOVA, $P < 0.05$). However, cell viability of the mHA treatment was significantly lower than the Ti treatment at day 7 (one-way ANOVA, $P < 0.05$, Fig. 6A). Cell viability in the Ag group was around 65% at days 1 and 4, and < 60% at day 7, although the time effect was not statistically significant. Cell viability in Ag + nHA treatment was

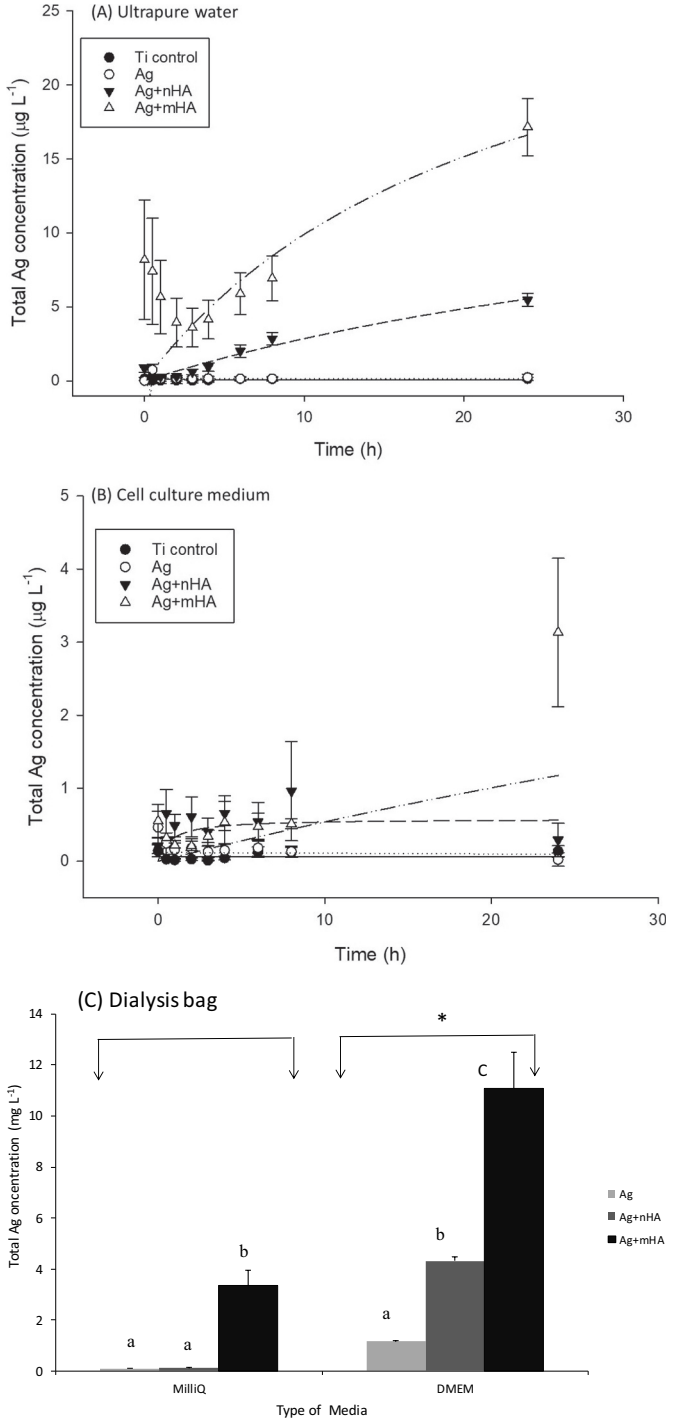

Fig. 3. Concentration of total silver released into the external media of beakers from titanium alloy discs during dialysis experiments in either, (A) ultrapure water, or (B) cell culture medium (DMEM +10% FBS + 1% antibiotics). Curves were fitted to a rectangular hyperbola function using SigmaPlot 13. Panel (C) shows the concentration of total silver remaining in the 4 mL solution in dialysis bags after 24 h. The treatment abbreviations are as explained in Table 2. Error bars represent S.E.M. (n = 3). In panel (C), * indicates a statistically significant difference between the ultrapure deioinsed water (MilliQ) and the cell culture medium (DMEM + 10% FBS + 1% antibiotics) in all treatments (coatings). Different letters between bars indicates a statistically significant difference between coatings within each media (one-way ANOVA, $P < 0.05$).

around 70%, with no significant differences between the time points (one-way ANOVA, $P < 0.05$). In contrast, there was a trend of decreasing in cell viability over time in Ag + mHA treatment, and by day 7 the cell viability was less than 60% of the reference control (Fig. 6A) and significantly less than the Ti treatment (one-way ANOVA, $P < 0.05$).

Enzyme activities were also measured in the homogenates. LDH enzyme activity was assessed in both cell homogenate after 7 days and cell culture medium at days 1, 4 and 7. The assay worked as expected, and LDH activity was detected in the cell homogenate in all treatment groups (Fig. 6B). Results showed that there was no significant difference in LDH activity between the treatments (Kruskal Wallis test, $P < 0.05$), with LDH activity being between 0.05-0.25 µmol min^{-1} mg^{-1} protein in all treatments (Fig. 6B). LDH activity in the external media was less than 5 nmol min^{-1} mL^{-1}. The ALP assay worked as expected, but low enzyme activity was detected in the cell homogenate. No significant differences between the treatments were observed (Kruskal Wallis test, $P < 0.05$). Values for the cell homogenates were between 0.05-0.3 nmol min^{-1} mg^{-1} protein (Fig. 6C).

3.6. Concentration of sodium, potassium, calcium and phosphorus in the external media

The concentration of electrolytes was measured in the external media over 7 days. Generally, electrolytes in the media did not show significant changes (Table 2). Na^+ and K^+ concentrations in the external media were stable and neither the time points nor the treatments showed any statistically significant changes (one-way ANOVA, $P < 0.05$). The values for Na^+ concentration were higher than 100 mmol L^{-1}, as expected, while K^+ concentrations were around 8 mmol L^{-1}. The Ca^{2+} concentrations remained around 1–2 mmol L^{-1} regardless of treatment. However, the Ca^{2+} concentration was significantly lower in Ag + nHA and nHA treatments compared to others at all time points (one-way ANOVA, $P < 0.05$), (Table 2). Phosphorus in the external media was around 1 mmol L^{-1} in all treatments, and the P concentration in the media was significantly lower in the HA-coated groups compared to all the others (one-way ANOVA, $P < 0.05$, Table 2). Moreover, nHA exhibited a significantly lower P concentration in the media compared to all the other treatments. Two-way ANOVA showed that there was both time and treatment effect on Ca^{2+} and P concentration ($P < 0.05$, Table 2).

4. Discussion

In this study, medical grade titanium alloy was successfully coated with Ag NPs by electroplating and then decorated with either a layer of nHA or mHA. As expected, the Ag coating alone was detrimental to cell attachment with fewer healthy cells observed. A top coat of either nHA and mHA improved cell health, with the Ag + nHA composite preferred by the cells. Cell health was corroborated by modest LDH activity in the cells and normal electrolyte concentrations. The presence of a background ALP activity indicated the cells were functional. However, the cells did accumulate some total Ag from all the treatments where an Ag coating was present. Dissolution experiments with the cell culture media demonstrated a slow release of dissolved silver, especially in the first 24 h of contact with a newly coated composite. This slow silver release did not affect the health of the osteoblasts and was interpreted as a desirable feature of the composite coatings; where in a clinical setting, the initial steps of osseointegration could proceed while providing antimicrobial conditions for infection control.

4.1. Characterisation and morphology of the coatings

The coating quality on the titanium alloy was assessed by SEM and EDS (Fig. 2). The silver electroplating method was successful and consistent with our previous work [9], forming a dense covering of Ag NPs of around 100 nm thick. The Ag NPs were formed from the electrochemical reduction of Ag^+ in $AgNO_3$ to Ag^0, and others have also used this approach to form silver nanocoatings (e.g. Ref. [22], on an

Table 2
Total concentration of Ag, Na^+, K^+, Ca^{2+} and P measured in the external media over 7 days when osteoblasts were grown on the titanium alloy with various coatings.

Element	Type of Coating	Day 1	Day 4	Day 7
Silver (mg L^{-1})	Reference control	0.057 ± 0.009 b	0.093 ± 0.009c	0.080 ± 0.007 b
	Ti	0.092 ± 0.013 b	0.073 ± 0.017 c	0.079 ± 0.014 b
	Ag	2.508 ± 0.419 a	3.552 ± 0.226 b	4.044 ± 0.527 a
	Ag + nHA	2.851 ± 0543 a	3.480 ± 0.640 b	2.608 ± 0.553 a
	Ag + mHA	2.039 ± 0.527 a	7.002 ± 2.375 a	3.841 ± 0.617 a
	nHA	0.150 ± 0.019 b	0.244 ± 0.60 c	0.276 ± 0.037 b
	mHA	0.290 ± 0.173 b	0.167 ± 0.021 c	0.138 ± 0.012 b
Sodium (mmol L^{-1})	Reference control	128.59 ± 3.48	163.69 ± 11.18	174.17 ± 8.58
	Ti	153.51 ± 9.15	179.83 ± 15.19	168.35 ± 8.38
	Ag	158.91 ± 9.63	163.73 ± 21.42	154.32 ± 10.15
	Ag + nHA	155.77 ± 9.79	167.27 ± 12.28	152.80 ± 4.82
	Ag + mHA	171.59 ± 19.37	209.98 ± 34.36	160.52 ± 9.58
	nHA	156.03 ± 9.37	171.53 ± 21.86	151.58 ± 9.73
	mHA	149.32 ± 8.64	171.08 ± 9.42	165.79 ± 14.33
Potassium (mmol L^{-1})	Reference control	6.04 ± 0.16	7.63 ± 0.55	8.02 ± 0.40
	Ti	7.17 ± 0.50	8.34 ± 0.73	7.73 ± 0.39
	Ag	7.57 ± 0.60	7.73 ± 1.04	7.08 ± 0.48
	Ag + nHA	7.52 ± 0.44	7.99 ± 0.53	7.09 ± 0.18
	Ag + mHA	8.17 ± 1.03	9.70 ± 1.65	7.38 ± 0.45
	nHA	7.36 ± 0.55	7.92 ± 0.99	7.09 ± 0.49
	mHA	6.96 ± 0.52	7.95 ± 0.49	7.50 ± 0.66
Calcium (mmol L^{-1})	Reference control	1.88 ± 0.04 a	2.11 ± 0.06 a	2.34 ± 0.13 a
	Ti	2.00 ± 0.06 a	2.28 ± 0.09 a	2.28 ± 0.10 a
	Ag	2.00 ± 0.04 a	2.09 ± 0.20 a	2.02 ± 0.06 ab
	Ag + nHA	0.72 ± 0.06 c	0.68 ± 0.05 b	0.75 ± 0.06 c
	Ag + mHA	1.61 ± 0.19 ab	1.14 ± 0.18 b	1.53 ± 0.15 b
	nHA	0.86 ± 0.04 c	0.87 ± 0.16 b	0.92 ± 0.15 c
	mHa	1.44 ± 0.93 b	1.78 ± 0.04 a	1.84 ± 0.08 ab
Phosphorus (mmol L^{-1})	Reference control	1.33 ± 0.08 a	1.46 ± 0.06 ab	1.65 ± 0.18 a
	Ti	1.36 ± 0.10 a	1.42 ± 0.10 ab	1.54 ± 0.16 a
	Ag	1.43 ± 0.09 a	1.32 ± 0.09 abc	1.35 ± 0.08 ab
	Ag + nHA	0.78 ± 0.09 bc	0.56 ± 0.03 bc	0.55 ± 0.04 c
	Ag + mHA	1.15 ± 0.08 ab	1.79 ± 0.52 a	1.02 ± 0.11 bc
	nHA	0.62 ± 0.03 c	0.48 ± 0.05 c	0.60 ± 0.03 c
	mHa	1.07 ± 0.11 ab	1.13 ± 0.07 abc	0.95 ± 0.10 bc

Data are mean ± S.E.M ($n = 6$). Different letters within the column in each element indicate a significant difference (one-way ANOVA or Kruskal Wallis test, $P < 0.05$). No label means there is no significant difference. The reference control are cells grown on a culture plate without any disc. Ti, titanium alloy disc alone. Ag, silver plated discs. Silver plated discs with a top coating of hydroxyapatite nanoparticles (Ag + nHA), or microparticles (Ag + mHA). Discs coated with hydroxyapatite nanoparticles alone (nHA), or microparticles alone (mHA).

Au–SiO_2 core/shell nanomaterial).

The HA coatings were also successfully applied to the silver plated titanium discs (Fig. 2). For both the mHA and nHA, the coatings showed densely packed particles of the relevant HA on the surface, but there were some notable differences between the nano and micron forms of HA. Firstly, the relatively large and spherical mHA particles formed a continuous layer, but inevitably, the geometry of the material enabled gaps in between particles, which allowed some silver release (see below). Besinis et al. [9] also observed this morphology. In contrast, for the more rod-like nHA the gaps in the material were much less. However, some cracks were observed on the surface of nHA-coated discs (Fig. 2). The formation of cracks after the sintering process is likely due to the difference in the coefficient of thermal expansion of HA, silver and titanium respectively [9]. Alternatively, nano HA shrinkage during the drying process is also suggested in the formation of cracks on the final surface [23].

The addition of nHA or mHA increased the surface roughness of the coatings compared to the Ag-coated Ti alloy alone. The values obtained here (0.2 to 2 μm) are considered to be a moderately rough surface, and these promoted attachment of healthy osteoblasts (Fig. 5). The roughness values here are also consistent with previous reports of these materials [9] and for Ti discs after polishing (e.g., 0.2 μm, [24]). The EDS analysis confirmed the elemental composition of the coatings was as expected, and also consistent with previous work [9].

4.2. Silver release from the coatings

The dialysis experiments (Fig. 3) showed some release of total dissolved Ag. The apparent Ag dissolution was much less in cell culture medium than ultrapure water (Fig. 3), and this is consistent with our previous findings where a sparingly soluble precipitate of AgCl particles (about 20 nm) is formed in the presence of millimolar concentrations of chloride ions [25]. These latter AgCl particles cannot penetrate the dialysis tubing (pore size < 2 nm), and so the total measured Ag remained inside the dialysis bag (Fig. 3C). Loza et al. [26] also reported some modest dissolution of Ag NPs in DMEM. This is also physiologically relevant since the cell culture medium intends to mimic the chemical composition of mammalian serum (e.g., nutrients, pH, electrolytes). Further leaching experiments with different modifications of the cell culture media and without the cells were also performed to understand the factors involved in the apparent dissolution (Table 1). The presence of 10% FBS in the DMEM caused almost 200 fold more silver release than DMEM alone. FBS is a heterogenous colloid with many different macromolecules including proteins. Any dissolved Ag^+ would avidly bind to the –SH groups on the amino acids (such as cysteine, [26]) in the cell culture media and/or serum, and to those –SH residues in the serum proteins. Steric hindrance may also entrap any AgCl particles, or the Ag NPs, within the colloidal structure of the protein macromolecules [27]. The effect of FBS has also been observed with TiO_2 nanoparticles where the presence of FBS caused 0.35% dissolution of Ti from TiO_2 nanoparticles compared to 0.02% without FBS [28].

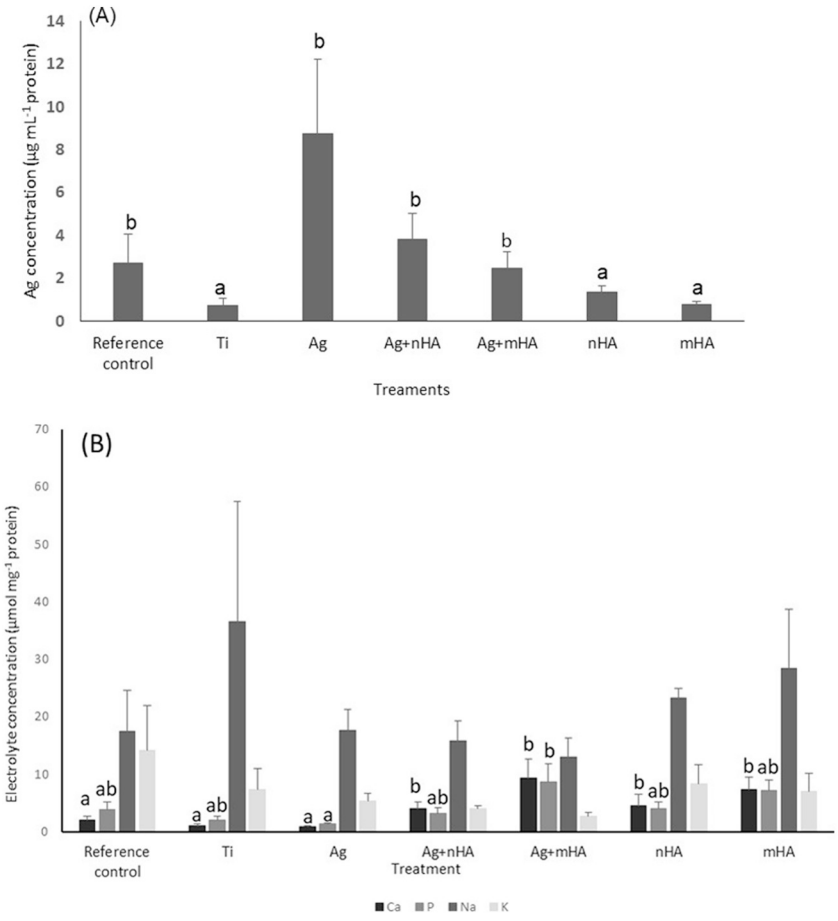

Fig. 4. Cell homogenate metal and electrolyte concentrations after 7 days. Concentration of (A) total silver, (B) Na^+, K^+, Ca^{2+} and P in the cell homogenates. Data are mean ± S.E.M., $n = 6$. The treatment abbreviations are as explained in Table 2. Different letters between the treatments indicate a significant difference (one-way ANOVA, or Kruskal Wallis test, $P < 0.05$).

It was a desired feature of the coating to release some silver to impart antimicrobial properties, but without causing toxicity to the osteoblasts. The silver concentrations in the media during the experiments were around 2–4 mg L^{-1} in the presence of the osteoblasts (Table 2). The concentration of total dissolved Ag to cause growth inhibition for the oral pathogen, *Streptococcus mutans*, is around

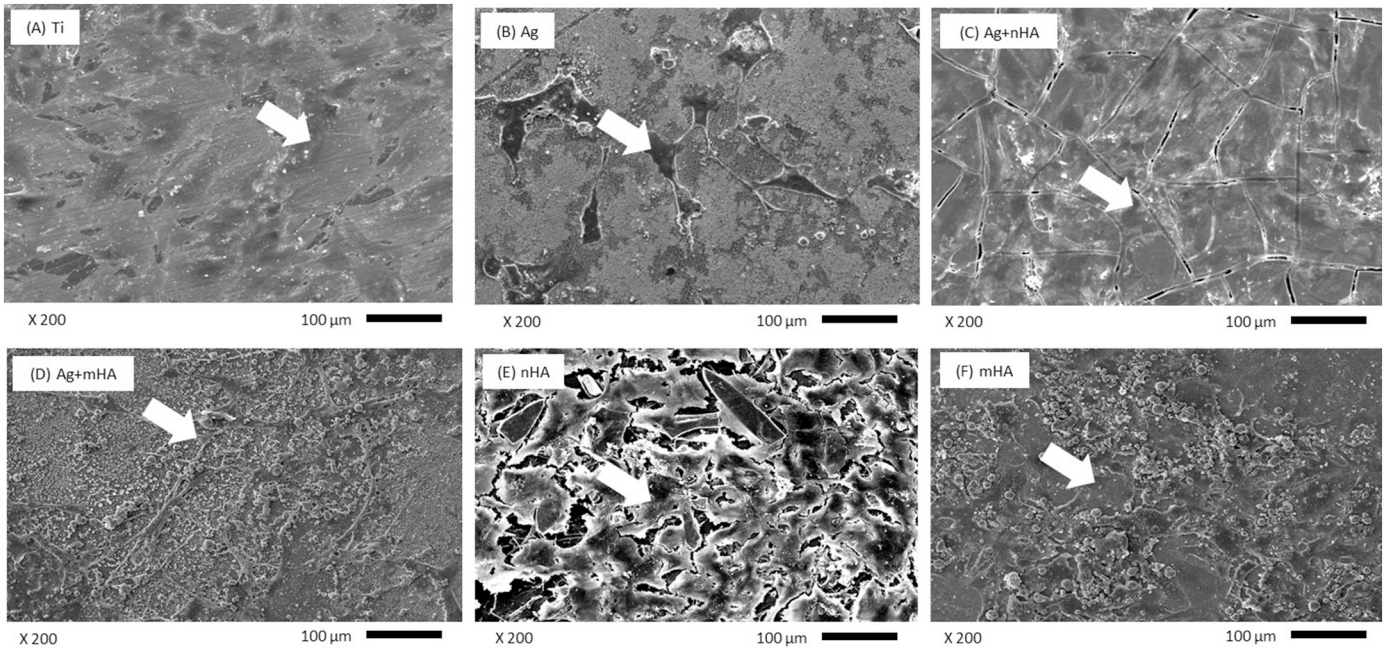

Fig. 5. SEM images of human primary osteoblast cells grown on titanium discs after 7 days. (A) uncoated Ti, (B) Ag, (C) Ag + nHA, (D) Ag + mHA, (E) nHA, (F) mHA. The treatment abbreviations are as explained in Table 2. Arrows show the cells grown on the surface. Note the membrane integrity, cell confluence and attachment with each other. Also, note the apparent cell shrinkage on Ag and Ag + mHA. All magnifications and scale bars are x200 and 100 µm respectively.

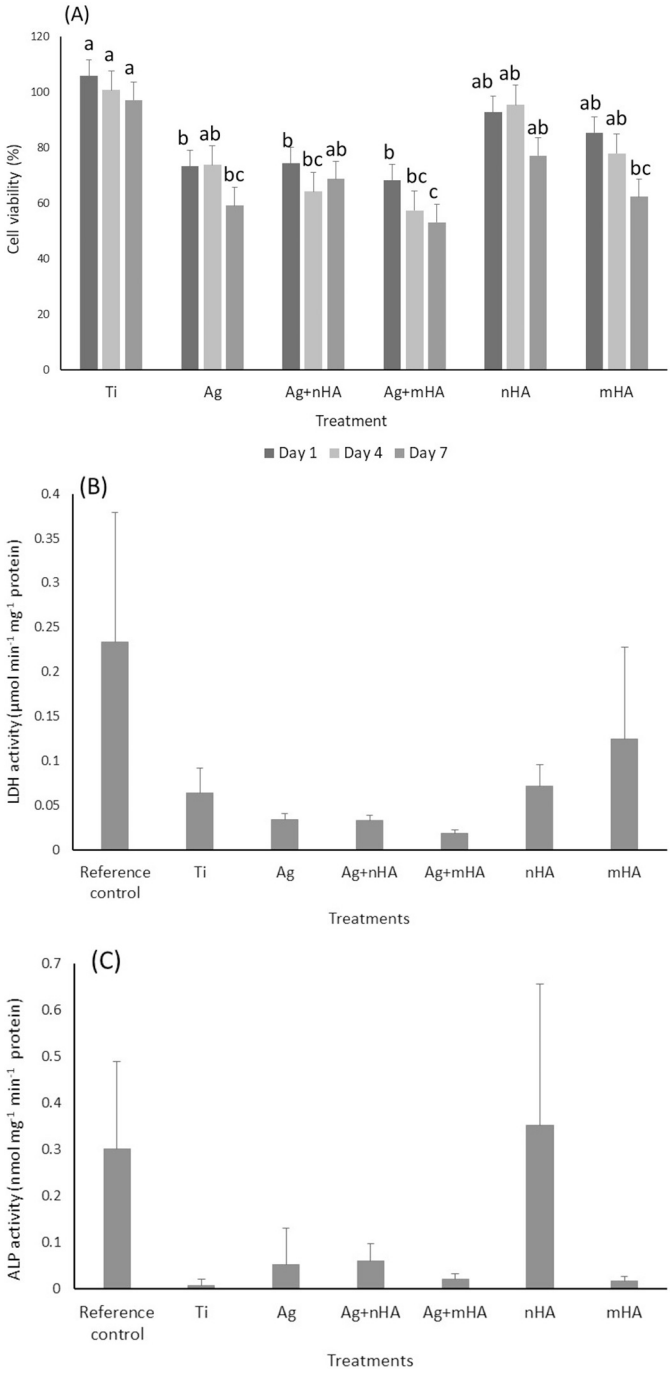

Fig. 6. Cell viability and cell homogenate biochemistry. (A) Cell viability over 7 days using an alamar blue assay. Different letters between the treatments within the same time point indicate a significant difference (one-way ANOVA, $P < 0.05$). There were no significant differences between the time points of any group (one-way ANOVA, $P > 0.05$). Panels (B) and (C) show lactate dehydrogenase (LDH) and alkaline phosphatase (ALP) specific activities in the cell homogenates at the end of the experiment (day 7). There were no statistically significant differences between the treatments for either enzyme (Kruskal Wallis test, $P > 0.05$). Data are mean ± S.E.M., ($n = 6$). The treatment abbreviations are as explained in Table 2.

$3.125\ mg\ L^{-1}$ [25], suggesting the desired biocidal properties were achieved in the cell culture media here. The antimicrobial properties of the coatings used here have also been demonstrated against *Streptococcus sanguinis* [9].

4.3. Biocompatibility of the coating with primary human osteoblast cells

Morphological examination at the end of the experiment confirmed the presence of mostly confluent and healthy osteoblasts on the Ti alloy, and in the presence of nano HA or micro HA without silver (Fig. 5). The cells had slightly less coverage and some cell shrinkage when grown directly on the Ag-coated Ti alloy discs (Fig. 5B), indicating that the cells were only tolerating direct contact with the Ag surface. In contrast, the cells in the Ag + nHA treatment were confluent and with good morphology (Fig. 5C) and while cells were also growing well on the Ag + mHA discs, they were slightly more sparse (Fig. 5D), indicating the Ag + nHA coating was the best substrate. The nHA, arguably, better resembles the mineral constituent of the living bone and thus will promote osteoblast cell attachment and growth [14,29]. While mHA consists of large particles that might interfere with cell-to-cell contact; thus despite having filopodia, these latter cells cannot attach with each other easily. Moreover, this would be exacerbated by the cell shrinkage observed on Ag + mHA (not seen on Ag + nHA, Fig. 5). Tian et al. [30] also found shrinkage of human bone marrow stem cells grown on a Ag NP-doped HA coating on titanium.

In addition to cell morphology, cell health was also assessed biochemically in the cell homogenates and with the alamar blue assay. The cells grown on Ti alloy showed 97% viability or more, indicating the cultures were healthy. As expected and consistent with the morphology above, osteoblasts were less tolerant of the silver coating, but the cells on the Ag + nHA coating showed 70% viability at the end of the experiment (Fig. 6A). LDH enzyme activity in the external media was low in all treatments, indicating no appreciable leak of the cell membrane. There was some LDH activity detected in the homogenates ($0.03–0.24\ \mu mol\ mg^{-1}$ protein, Fig. 6B) and this is a typical background for cell cultures (e.g., Ref. [31]). The absence of elevated LDH activity also confirmed the cells were not under metabolic anaerobic stress. There were also no statistically significant changes in the Na^+ or K^+ concentrations in the homogenates (Fig. 4) that would infer osmotic distress or cell lysis. Ca^{2+} and P levels in the cell homogenate were higher in HA coated discs compared to the others, as expected, likely due to the Ca^{2+} and P adsorption from the media to the cells. This phenomenon is also well-known for HA coatings where the –OH group in the HA can attract Ca^{2+} and P from the external media to form calcium hydroxide and calcium phosphate hydroxide [32]. However, this did not impact on cell health as Ca^{2+} or P remained in nutritional excess in the media (Table 2). The ALP activity was also measured (Fig. 6C). Alkaline phosphatase activity was low at around $0.02–0.32\ nmol\ mg^{-1}$ protein. However, this background is expected since the ALP activity is mainly induced at a later stage of the cell differentiation process [33]. Nonetheless, the values here show the cells are functional with respect to the role of ALP activity in bone formation, and the values are broadly similar to those reported for osteoblasts (e.g., $0.5–5\ nmol\ mg^{-1}$ protein, [34]). Taken together, the cell morphology, the viability assay, and the biochemistry indicated that the cells were healthy, despite silver exposure.

The exposure to Ag was confirmed by the measured concentrations of total Ag in the media over 7 days (Table 2) and in the cell homogenates (Fig. 4). As expected, the treatments without added Ag had a trace but detectable concentration of total Ag ($< 0.1\ \mu g\ mg^{-1}$ protein). Culturing the cells on the various Ag-containing coatings significantly elevated the Ag concentrations in the final cell homogenates (Fig. 4), but without overtly affecting cell health. Despite attempts to carefully wash the cells, it is possible that some of the apparent Ag accumulation is on, not inside, the cells. However, for dissolved metals and nanomaterials, the surface adsorbed fraction is around one fifth or less of the apparent accumulation (e.g., TiO_2 NPs, [35]). Most of the measured Ag in the homogenates here is therefore likely to arise from direct exposure of the cells.

Ag NPs can, in theory, mediate toxicity through the dissolution of dissolved Ag^+ into the media, or by direct contact toxicity with perhaps

a local dissolution of ions at the cell surface [7]. The absence of free ion toxicity in the cell culture media can be explained by the formation of sparingly soluble AgCl and the chelation of any remaining Ag by amino acids and/or serum proteins (as discussed above). The dialysis experiments suggest the cells were mostly exposed to particulate Ag, but the form inside the cells requires further investigation. Nonetheless, other researchers have also reported the biocompatibility of Ag-containing composites. For example [36], demonstrated the viability of human fibroblasts over 7 days on coatings made of titania nanotubes anodised with Ag, despite an estimated release of 1 mg L^{-1} of total silver into the cell culture media.

4.4. Clinical perspective and conclusions

Any new implant containing nanomaterials should be preferably be more effective than the existing product, show biocompatibility with human tissues, and be safe in the long term [37]. Our previous work has already demonstrated the antimicrobial powers of coatings containing Ag and HA [9], and here we demonstrate biocompatibility over 7 days with the human osteoblasts that are crucial to osseointegration and the success of the implant for the patient. The Ag + nHA coating is the preferred substrate. Further experiments are needed over several weeks to confirm if the cells will mature and can mineralise to produce new bone on the surface of the discs. Only then could further clinical trials with human volunteers be considered for this promising material.

Data availability

The raw data in this project is not publically available to share for legal, and other reasons relating to ongoing studies, but the corresponding author will consider requests for data collaborations for academic (not for profit) purposes.

Acknowledgements

This work was partly funded by HCDP programme of Kurdistan regional government to Ranj Salaie. Technical support from the Plymouth Electron Microscopy Centre, and for cell culture and trace metal analysis at Plymouth University is acknowledged.

Appendix A. Supplementary data

Supplementary data to this article can be found online at https://doi.org/10.1016/j.msec.2019.110210.

References

[1] W. Chee, S. Jivraj, Failures in implant dentistry, Br. Dent. J. 202 (3) (2007) 123.
[2] S. Hadi, N. Ashfaq, A. Bey, S. Khan, Biological factors responsible for failure of osseointegration in oral implants, Biol. Med. 3 (2) (2011) 164–170.
[3] L. Zhao, P.K. Chu, Y. Zhang, Z. Wu, Antibacterial coatings on titanium implants, J. Biomed. Mater. Res. B. 91B (1) (2009) 470–480.
[4] S. Sakka, P. Coulthard, Implant failure: etiology and complications, Med. Oral Patol. Oral Cir. Bucal 16 (1) (2011) e42–e44.
[5] V. Alt, A. Bitschnau, J. Österling, A. Sewing, C. Meyer, R. Kraus, S.A. Meissner, S. Wenisch, E. Domann, R. Schnettler, The effects of combined gentamicin–hydroxyapatite coating for cementless joint prostheses on the reduction of infection rates in a rabbit infection prophylaxis model, Biomaterials 27 (26) (2006) 4627–4634.
[6] L. Harris, L. Mead, E. Müller-Oberländer, R. Richards, Bacteria and cell cytocompatibility studies on coated medical grade titanium surfaces, J. Biomed. Mater. Res. A. 78 (1) (2006) 50–58.
[7] B. Reidy, A. Haase, A. Luch, K.A. Dawson, I. Lynch, Mechanisms of silver nanoparticle release, transformation and toxicity: a critical review of current knowledge and recommendations for future studies and applications, Materials 6 (6) (2013) 2295–2350.
[8] A. Besinis, T. De Peralta, R.D. Handy, Inhibition of biofilm formation and antibacterial properties of a silver nano-coating on human dentine, Nanotoxicology 8 (7) (2014) 745–754.
[9] A. Besinis, S.D. Hadi, H. Le, C. Tredwin, R. Handy, Antibacterial activity and biofilm inhibition by surface modified titanium alloy medical implants following application of silver, titanium dioxide and hydroxyapatite nanocoatings, Nanotoxicology 11 (3) (2017) 327–338.
[10] Z. Meran, A. Besinis, T. De Peralta, R.D. Handy, Antifungal properties and biocompatibility of silver nanoparticle coatings on silicone maxillofacial prostheses *in vitro*, J. Biomed. Mater. Res. B. 106 (3) (2018) 1038–1051.
[11] A. Ivask, I. Kurvet, K. Kasemets, I. Blinova, V. Aruoja, S. Suppi, H. Vija, A. Käkinen, T. Titma, M. Heinlaan, Size-dependent toxicity of silver nanoparticles to bacteria, yeast, algae, crustaceans and mammalian cells *in vitro*, PLoS One 9 (7) (2014) e102108.
[12] J.R. Woodard, A.J. Hilldore, S.K. Lan, C. Park, A.W. Morgan, J.A.C. Eurell, S.G. Clark, M.B. Wheeler, R.D. Jamison, A.J.W. Johnson, The mechanical properties and osteoconductivity of hydroxyapatite bone scaffolds with multi-scale porosity, Biomaterials 28 (1) (2007) 45–54.
[13] M. Hasegawa, T.-A. Kudo, H. Kanetaka, T. Miyazaki, M. Hashimoto, M. Kawashita, Fibronectin adsorption on osteoconductive hydroxyapatite and non-osteoconductive α-alumina, Biomed. Mater. 11 (4) (2016) 045006.
[14] G. Mendonça, D.B. Mendonça, F.J. Aragao, L.F. Cooper, Advancing dental implant surface technology–from micron-to nanotopography, Biomaterials 29 (28) (2008) 3822–3835.
[15] F. Bezerra, M.R. Ferreira, G.N. Fontes, C.J. da Costa Fernandes, D.C. Andia, N.C. Cruz, R.A. da Silva, W.F. Zambuzzi, Nano hydroxyapatite-blasted titanium surface affects pre-osteoblast morphology by modulating critical intracellular pathways, Biotechnol. Bioeng. 114 (8) (2017) 1888–1898.
[16] Z. Shi, X. Huang, Y. Cai, R. Tang, D. Yang, Size effect of hydroxyapatite nanoparticles on proliferation and apoptosis of osteoblast-like cells, Acta Biomater. 5 (1) (2009) 338–345.
[17] S.L.K. Hung, C. Shih, Y. Yang, H. Feng, Y. Lin, Titanium surface modified by hydroxyapatite coating for dental implants, Surf. Coat. Technol. 231 (2013) 337–345.
[18] J.-K. Lee, D.-S. Choi, I. Jang, W.-Y. Choi, Improved osseointegration of dental titanium implants by TiO_2 nanotube arrays with recombinant human bone morphogenetic protein-2: a pilot *in vivo* study, Int. J. Nanomed. 10 (2015) 1145.
[19] T. Albrektsson, A. Wennerberg, Oral implant surfaces: Part 1-review focusing on topographic and chemical properties of different surfaces and *in vivo* responses to them, Int. J. Prosthod. 17 (5) (2004) 536–543.
[20] R. Handy, F. Eddy, G. Romain, *In vitro* evidence for the ionoregulatory role of rainbow trout mucus in acid, acid/aluminium and zinc toxicity, J. Fish Biol. 35 (5) (1989) 737–747.
[21] D.T. Plummer, An Introduction to Practical Biochemistry, McGraw Hill, London, 1971, pp. 288–289.
[22] D. Li, D.-W. Li, Y. Li, J.S. Fossey, Y.-T. Long, Cyclic electroplating and stripping of silver on $Au@SiO_2$ core/shell nanoparticles for sensitive and recyclable substrate of surface-enhanced Raman scattering, J. Mater. Chem. 20 (18) (2010) 3688–3693.
[23] M. Mahé, J.-M. Heintz, J. RÖdel, P. Reynders, Cracking of titania nanocrystalline coatings, J. Eur. Ceram. Soc. 28 (10) (2008) 2003–2010.
[24] G. Giavaresi, M. Fini, A. Cigada, R. Chiesa, G. Rondelli, L. Rimondini, P. Torricelli, N.N. Aldini, R. Giardino, Mechanical and histomorphometric evaluations of titanium implants with different surface treatments inserted in sheep cortical bone, Biomaterials 24 (9) (2003) 1583–1594.
[25] A. Besinis, T. De Peralta, R.D. Handy, The antibacterial effects of silver, titanium dioxide and silica dioxide nanoparticles compared to the dental disinfectant chlorhexidine on *Streptococcus mutans* using a suite of bioassays, Nanotoxicology 8 (1) (2014) 1–16.
[26] K. Loza, J. Diendorf, C. Sengstock, L. Ruiz-Gonzalez, J. Gonzalez-Calbet, M. Vallet-Regi, M. KÖller, M. Epple, The dissolution and biological effects of silver nanoparticles in biological media, J. Mater. Chem. B. 2 (12) (2014) 1634–1643.
[27] J.R. Lead, G.E. Batley, P.J. Alvarez, M.N. Croteau, R.D. Handy, M.J. McLaughlin, J.D. Judy, K. Schirmer, Nanomaterials in the environment: behavior, fate, bioavailability, and effects - an updated review, Environ. Toxicol. Chem. 37 (2018) 2029–2063.
[28] J. Shi, H.L. Karlsson, K. Johansson, V. Gogvadze, L. Xiao, J. Li, T. Burks, A. Garcia-Bennett, A. Uheida, M. Muhammed, S. Mathur, Microsomal glutathione transferase 1 protects against toxicity induced by silica nanoparticles but not by zinc oxide nanoparticles, ACS Nano 6 (3) (2012) 1925–1938.
[29] H. Wang, Y. Li, Y. Zuo, J. Li, S. Ma, L. Cheng, Biocompatibility and osteogenesis of biomimetic nano-hydroxyapatite/polyamide composite scaffolds for bone tissue engineering, Biomaterials 28 (22) (2007) 3338–3348.
[30] W.C.B. Tian, D. Yu, Y. Lei, Q. Ke, Y. Guo, Z. Zhu, Fabrication of silver nanoparticle-doped hydroxyapatite coatings with oriented block arrays for enhancing bactericidal effect and osteoinductivity, J. Mech. Behav. Biomed. 61 (2016) 345–359.
[31] C. Gitrowski, A.R. Al-Jubory, R.D. Handy, Uptake of different crystal structures of TiO_2 nanoparticles by Caco-2 intestinal cells, Toxicol. Lett. 226 (3) (2014) 264–276.
[32] I. Harding, N. Rashid, K. Hing, Surface charge and the effect of excess calcium ions on the hydroxyapatite surface, Biomaterials 26 (34) (2005) 6818–6826.
[33] A. Yamaguchi, T. Komori, T. Suda, Regulation of osteoblast differentiation mediated by bone morphogenetic proteins, hedgehogs, and Cbfa1, Endocr. Rev. 21 (4) (2000) 393–411.
[34] G. Kim, C.-H. Kim, J. Park, K.-U. Lee, C. Park, Effects of vitamin B12 on cell proliferation and cellular alkaline phosphatase activity in human bone marrow stromal osteoprogenitor cells and UMR106 osteoblastic cells, Metabolism 45 (12) (1996) 1443–1446.
[35] A.R. Al-Jubory, R.D. Handy, Uptake of titanium from TiO_2 nanoparticle exposure in the isolated perfused intestine of rainbow trout: nystatin, vanadate and novel CO_2-sensitive components, Nanotoxicology 7 (8) (2013) 1282–1301.
[36] S. Mei, H. Wang, W. Wang, L. Tong, H. Pan, C. Ruan, Q. Ma, M. Liu, H. Yang, L. Zhang, Antibacterial effects and biocompatibility of titanium surfaces with graded silver incorporation in titania nanotubes, Biomaterials 35 (14) (2014) 4255–4265.
[37] A. Besinis, T. De Peralta, C.J. Tredwin, R.D. Handy, Review of nanomaterials in dentistry: interactions with the oral microenvironment, clinical applications, hazards, and benefits, ACS Nano 9 (3) (2015) 2255–2289.